



# Application of the analytical hierarchy process (AHP) for flood susceptibility mapping using GIS techniques in Thamirabarani river basin, Srivaikundam region, Southern India

Richard Abishek Selvam<sup>1,2</sup> · Antony Ravindran Antony Jebamalai<sup>1</sup>

Received: 23 October 2022 / Accepted: 18 May 2023 / Published online: 30 May 2023  
© The Author(s), under exclusive licence to Springer Nature B.V. 2023

## Abstract

Flood susceptibility mapping is required for assessing flood risk areas and developing flood prevention techniques. The Thamirabarani river basin, a flood-prone area in the Tamil Nadu region of Srivaikundam, was investigated. Flood risk assessment using a composite risk and vulnerability index is a well-established tool that plays an important role in the development of flood risk reduction schemes. The present research is an attempt to analyze flood risk using analytical hierarchy procedures in a geographic information system context, which includes flood hazard components and susceptibility indicators. Geographic information system (GIS) are currently a trusted and useful tool for defining flood susceptibility maps at various spatial scales. The accuracy of various GIS-based flood risk assessment techniques is compared in this article. Land use and land cover, drainage density, topographic wetness index, distance from rivers, river length, slope, DEM, and rainfall were the eight foundation layers that were generated from the geographical database. All of the thematic layers and the resulting flood frequency map were combined to create the flood susceptibility using a GIS platform. Flood-vulnerable areas have been classified as very low class (1.7%), low class (26.3%), medium class (42.1%), high class (24%), and very high class (5.9%). The flood susceptibility study with this model will be a very beneficial and efficient tool for creating flood mitigation measures, according to local government administrators, researchers, and planners.

**Keywords** Flood susceptibility · AHP method · Remote sensing · GIS · Srivaikundam region

---

✉ Richard Abishek Selvam  
richardabishek9710@gmail.com

<sup>1</sup> PG and Research Department of Geology, V.O. Chidambaram College, Thoothukudi 628008, India

<sup>2</sup> Affiliated with Manonmaniam Sundaranar University, Tirunelveli, India

## 1 Introduction

Flooding is described as an increase in the level of rivers and floodways, flowing water, and covering lands along the river, in accordance with Ahmed et al. (2021). It goes without saying that human activities like population growth and rapid urban and rural development have increased the risk of flooding. Elkhrachy (2015) Floods are regarded as the worst climate disasters in history in terms of fatalities and property loss. Flooding occurs naturally on the flood plains, which are disaster-prone, and is a situation that results when land that is often dry is covered with water from a river overflowing or heavy rain. Floods are generally generated by two key components, human and man-made, which are definitely responsible for the formation and continual occurrence of floods in the environment and, at any time, negatively affect the ecosystem at large. Natural disasters can be efficiently monitored with the help of current technology and information systems developed by Hong et al. (2018). Floods can be beneficial in that they can shift fertile soil to farmlands and disperse fish to smaller bodies of water, but they can also be very devastating to the places nearby. Bajabaa et al. (2014) One of Tamil Nadu permanent rivers, the Thamirabarani, is continually being examined. Flash flood management studies must contain accurate flash flood susceptibility maps from policymakers in order to better reduce the effects of flash floods and methodically develop the area. Flood hazard management is a process in which multiple authorities strive to reduce human society current and future susceptibility to natural disasters, as examined by Malik et al. (2020). The purpose of this study is to map the spatial variation of the Thamirabarani river basin in the Thoothukudi area of Tamil Nadu. Flood mapping can help with decision making in the aftermath of such occurrences by facilitating risk management, near-real-time forecasting, and land use and land cover management (LU/LC). Floods have thus been largely delimited using geographic information system (GIS) or remote sensing (RS) data to examine the extent of flooded areas (Swain et al. 2020). GIS is a useful tool for visualizing geographical variation and is important for monitoring environmental changes Khosravi et al. (2016). The identification and selection of flooding causation elements such as slope, runoff, drainage network density, distance from drainage channel, land use and cover, surface roughness, rainfall rate, and geology are based on their significance and contribution to the flood carried out by Abdel Hamid et al. (2020). Saaty (1980) created the analytical hierarchy process (AHP), which is recognized as a mathematical method for making multi-criteria decisions. The analytical hierarchy process (AHP) in a specific scenario. It's used to calculate the weights of various themes and classes in order to identify the groundwater vulnerable zone. In the research region, a linear combination of these weights is employed to create five distinct groundwater-vulnerable zones. The most widely used technique is the analytical hierarchy process (AHP) developed by Ghosh and Kar (2018), which has been utilized to create a one-of-a-kind decision-making framework for flood susceptibility mapping. Natarajan et al. (2021). The methodological framework adopted formulates the cumulative character of each criterion, which is useful for creating flood data on a local, regional, and national scale. The purpose of this study is to define and classify the flood vulnerability and risk assessment zones in the flood susceptibility map using the analytical hierarchy process (AHP) and geographic information system (GIS).

## 2 Study area

The study region was situated at 8° 38 40.3 N latitude and 78° 06 45.3 E longitude. The length of the Thamirabarani river is 128 km, and the tributaries of the river pattern are Karaiyar, Servalar, Gadanathi, Chittar, Manimutharu, and Pachaiyar. The Srivaikundam region generally experiences subtropical climates. The region is characterized by two types of monsoons, including the southwest monsoon from June to September and the northeast monsoon from October to December. The region’s average annual temperature ranges from 23 to 27 degrees Celsius. The northeast monsoon brings the most precipitation (October and December). The geologic strata include tertiary deposits, quaternary alluvium, Terry Sands (sand dunes), and zones of weathering in gneisses and charnockite. The principal land uses in this region, excluding human settlements and water bodies, are agricultural land, badlands, and salt water (Fig. 1). The Thamirabarani Delta is underlain by Archean rocks containing gneisses, granite, and charnockite.

## 3 Material and methods

The methods used during the current investigation are shown in the flowchart in Fig. 2. Identification of flood-prone locations utilizing the GIS environment is the primary objective of this study (Hammami et al. 2019). Initially, many data sources, such as satellite images, spatial data, and geological and topographic maps, were used and introduced in ArcGIS. But because of their significance in choosing the flood region, a particular set of criteria was included in the current study.

The decision problem must be defined as the first step in the AHP approach. Making a pairwise comparison matrix is the second stage in the process (Yaralioglu 2004). At

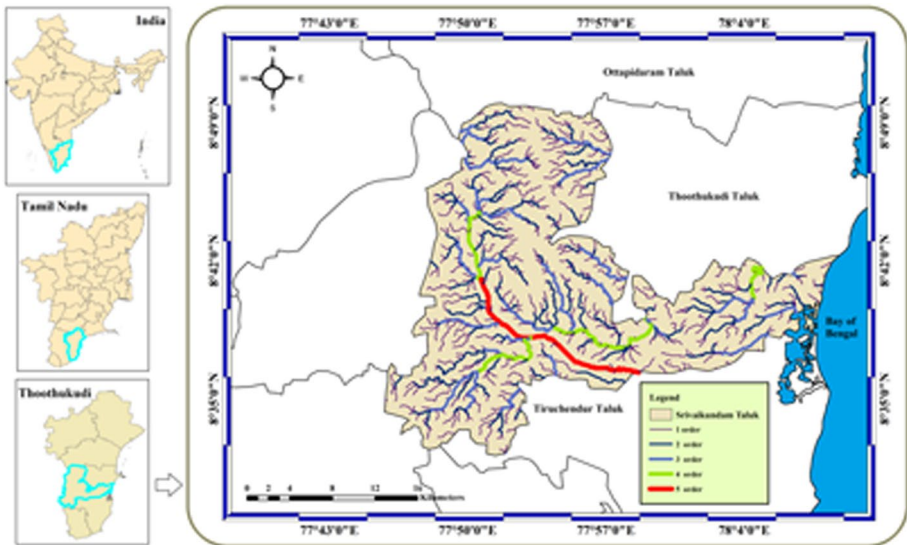
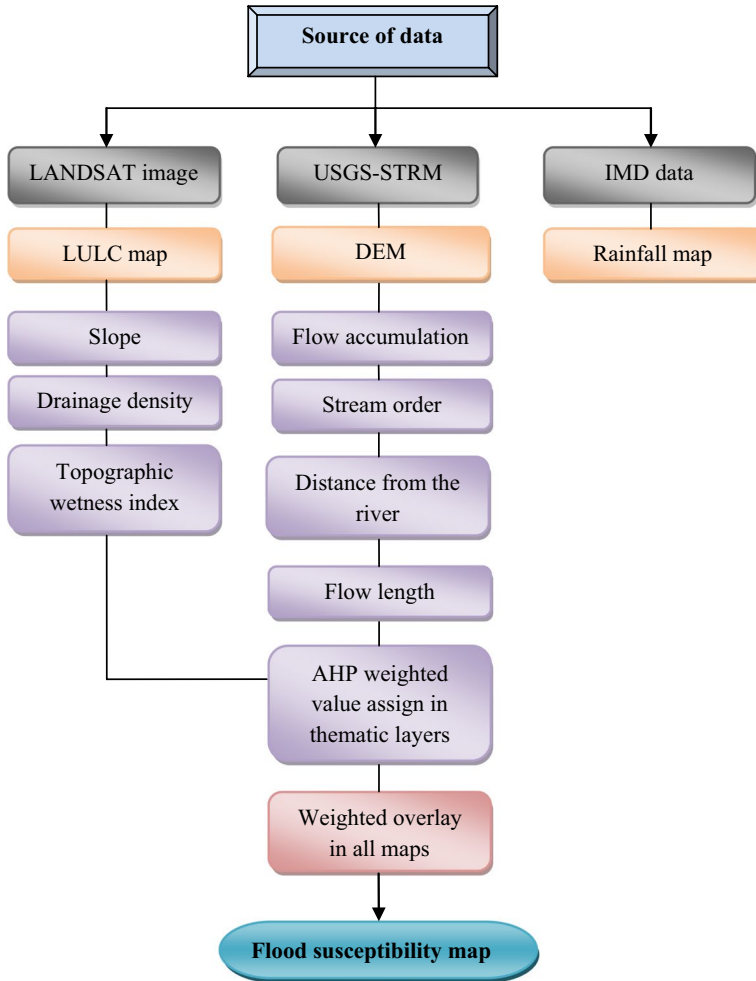


Fig. 1 Location and stream order flow map of the Thamirabarani river basin in Srivaikundam region



**Fig. 2** Flow chart of flood susceptibility map by GIS method

**Table 1** The fundamental scale of AHP (Saaty 1980)

Intensity importance	Description
1	Equal importance
3	Moderate importance
5	Strong importance
7	Very strong importance
9	Extreme importance
2, 4, 6, 8	Intermediate values
Reciprocals	Inverse comparison

**Table 2** Saaty’s ratio index for different values of *N* (Saaty 1980)

<i>N</i>	1	2	3	4	5	6	7	8	9	10
RI	0	0	0.58	0.89	1.12	1.24	1.32	1.41	1.45	1.49

this point, a pairwise comparison matrix with  $n * n$  elements has been created using the conditioning factors. The Saaty (1980) important value scale is used (Table 1). Each factor was then assigned an arithmetic number between 1 and 9 based on its relevance in relation to the other factors with which it was associated. A weight value based on its relative importance was assigned to each aspect in order to undertake a thorough analysis of how each component affected flood generation in the research region. The AHP approach was employed to standardize these weights. The model was implemented into a GIS system to produce a flood risk map, as studied by Dandapat and Panda (2017). Next, the consistency ratio (CR) was determined. If the CR ratio exceeds 0.1, the assessments can be too inconsistent to be trusted. However, when CR is equal to 0, the results seem to be entirely consistent (Elkhrachy 2015). Finally, the consistency index and consistency ratio are calculated using the following formulas to make sure that the analysis is stable. The random index (RI) equation is divided by the consistency index (CI) (1) to get the value of CR in Table 2. Generally, a CR of 0.10 or less (for  $n > 5$ ); 0.09 or less (for  $n = 4$ ); 0.05 or less (for  $n = 3$ ), is considered acceptable

$$\text{Consistency Index (CI)} = \frac{\text{Max principal Eigen value } (\lambda) - \text{Number of factors } (n)}{\text{Number of factors } (n) - 1} \tag{1}$$

$$\text{Consistency ratio (CR)} = \frac{\text{Consistency Index (CI)}}{\text{Random consistency Index (RI)}} \tag{2}$$

$$\text{Consistency Index (CI)} = \frac{8 - 8}{9 - 1} = \frac{0}{8}$$

$$\text{Consistency Index (CI)} = 0$$

**Table 3** AHP matrix for flood susceptibility zone

Thematic layer	Assigned weight	LCLU	Drainage density	TWI	River length	Distance from the river	Slope	DEM	Rainfall
LCLU	8	8/8	8/7	8/6	8/5	8/4	8/3	8/2	8/1
Drainage density	7	7/8	7/7	7/6	7/5	7/4	7/3	7/2	7/1
TWI	6	6/8	6/7	6/6	6/5	6/4	6/3	6/2	6/1
Distance from the river	5	5/8	5/7	5/6	5/5	5/4	5/3	5/2	5/1
River length	4	4/8	4/7	4/6	4/5	4/4	4/3	4/2	4/1
Slope	3	3/8	3/7	3/6	3/5	3/4	3/3	3/2	3/1
DEM	2	2/8	2/7	2/6	2/5	2/4	2/3	2/2	2/1
Rainfall	1	1/8	1/7	1/6	1/5	1/4	1/3	1/2	1/1

**Table 4** Pairwise comparison matrix of 8 criteria for the AHP process

Suitability criterion	LCLU	Drainage density	TWI	River length	Distance from the river	Slope	DEM	Rainfall
LCLU	1	1.1	1.3	1.6	2	2.7	4	8
Drainage density	0.9	1	1.2	1.4	1.75	2.3	3.5	7
TWI	0.8	0.9	1	1.2	1.5	2	3	6
Distance from the river	0.6	0.7	0.8	1	1.25	1.7	2.5	5
River length	0.5	0.6	0.7	0.8	1	1.3	2	4
Slope	0.4	0.4	0.5	0.6	0.75	1	1.5	3
DEM	0.3	0.3	0.3	0.4	0.5	0.7	1	2
Rainfall	0.1	0.1	0.2	0.2	0.25	0.3	0.5	1

$$\text{Consistency ratio (CR)} = \frac{0}{1.41} = 0$$

= 0 Since 0 < 0.1, assuming that the pairwise comparisons are reasonably consistent, weights of 0.20, 0.18, 0.16, 0.13, 0.09, 0.07, 0.04, and 0.02 (i.e., 5%, 22%, 10%, 15%, 12%, 20%, and 14%, respectively) can be assigned to the variables lithology, LULC, drainage density, TWI (topographic wetness index), distance from river, river length, slope, DEM, and rainfall. The inputs, which are the classified maps, were subjected to computational weights. At this stage, the problem is re-entered into the GIS system, and classes are created by combining weighted values. The values for various themes are shown in Tables 3 and 4.

## 4 Result and discussion

The multiple thematic layers were constructed using satellite images of digital elevation models (DEM), existing data/maps, and field verification using remote sensing and GIS techniques (Das 2020) to establish the flood risk zone in the study area. The relative importance of these links between the influencing factors reveals how each one reacts to the presence of the study region. In a GIS setting, these factors are used in conjunction with risk zone weights to calculate the flood risk zone (Tables 5, 6).

### 4.1 Land use and land cover map

According to human activities, which are primarily connected to the occurrence and development of water in the ground, land use and land cover show the coverage and natural characteristics of the land. The varied land use and land cover patterns discovered in the research area. The land use and land cover map were made using GIS software and data from LANDSAT-8 satellite pictures obtained from the ESRI website. This analysis of land use and land cover during this time reveals typical alterations in coverage parameters that were influenced by the local economic crisis. This is plainly seen in the increasing conversion of agricultural lands to development lands. They are divided into the categories of,

**Table 5** Determining the relative criterion weights

Suitability criterion	LCLU	Drainage density	TWI	River length	Distance from the river	Slope	DEM	Rainfall	Weighted sum value	Criteria weight	$\lambda = \text{Weighted sum value/criteria weight}$
LCLU	0.22	0.22	0.221	0.224	0.22	0.216	0.24	0.24	1.801	0.22	8.19
Drainage density	0.198	0.2	0.204	0.196	0.1925	0.184	0.21	0.21	1.5945	0.2	7.97
TWI	0.176	0.18	0.17	0.168	0.165	0.16	0.18	0.18	1.379	0.17	8.11
River length	0.132	0.14	0.136	0.14	0.1375	0.136	0.15	0.15	1.1215	0.14	8.01
Distance from the river	0.11	0.12	0.119	0.112	0.11	0.104	0.12	0.12	0.915	0.11	8.32
Slope	0.088	0.08	0.085	0.084	0.0825	0.08	0.09	0.09	0.6795	0.08	8.49
DEM	0.066	0.06	0.051	0.056	0.055	0.056	0.06	0.06	0.464	0.06	7.73
Rainfall	0.022	0.02	0.034	0.028	0.0275	0.024	0.03	0.03	0.2155	0.03	7.18
Total										1	64.01

**Table 6** Assigned weight rankings and overall of the sub-classes of each thematic map-related classes for flood analysis

Thematic layer	Factors	Rank	Weight	Overall
LCLU	Waters	5	24	120
	Trees	4		96
	Flooded vegetation	3		72
	Crops	3		72
	Built area	2		48
	Bare ground	1		24
	Rangeland	1		24
TWI	Very low	1	20	20
	Low	2		40
	Moderate	3		60
	High	4		80
	Very high	5		100
Drainage density	Very low	1	18	18
	Low	2		36
	Moderate	3		54
	High	4		72
	Very high	5		90
Distance from the river	Very low	1	15	15
	Low	2		30
	Moderate	3		45
	High	4		60
	Very high	5		75
River length	Very low	1	11	11
	Low	2		22
	Moderate	3		33
	High	4		44
	Very high	5		55
Slope	Very low	1	6	6
	Low	2		12
	Moderate	3		18
	High	4		24
	Very high	5		30
DEM	Very low	1	3	3
	Low	2		6
	Moderate	3		9
	High	4		12
	Very high	5		15
Rainfall	Very low	1	3	3
	Low	2		6
	Moderate	3		9
	High	4		12
	Very high	5		15



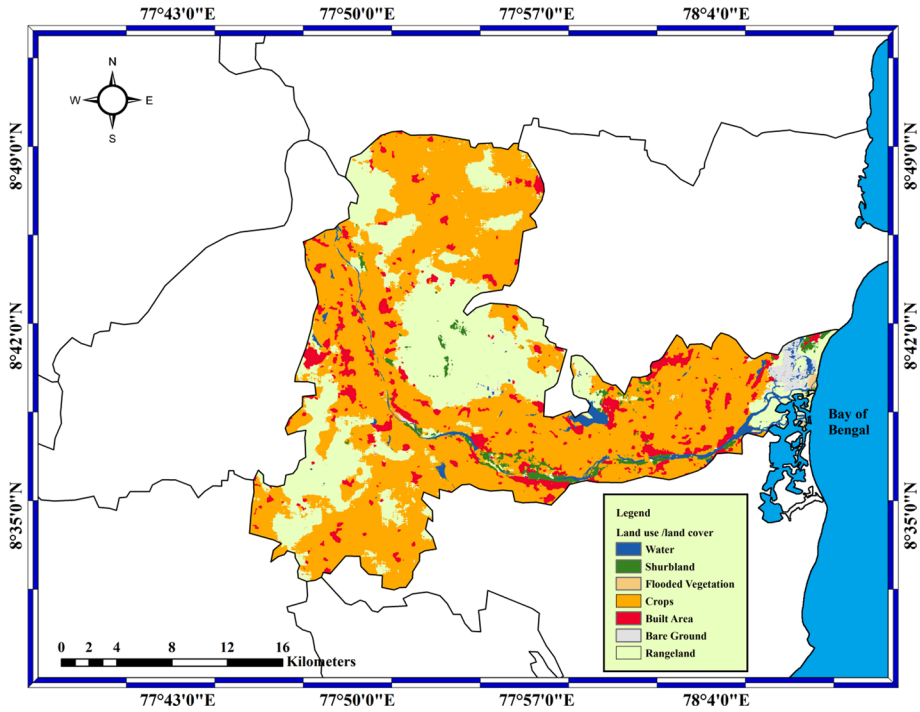


**Fig. 3** Land use and land cover map of Srivaikundam region

including water bodies, mud land, vegetation, settlements, arid terrain, and shrub cover. The kind of land use, area covered, infiltration rate, and surface water storage capacity all affect the weight. A high priority is given to agricultural land and water bodies, while communities and uninhabited places are given a low priority due to the water’s moderate ability to grip onto objects. The land use and land cover of the area are divided into categories in order to assign ranks. It varies from extremely low to extremely high (see Fig. 3). The percentage coverage of each kind is as follows: 2.1% for water, 1.6% for shrubland, 0.1% for rangeland, 59.9% for swamps, 7.4% for crops, 0.9% for built-up areas, and 27.6% for barren terrain.

**4.2 Drainage density map**

The drainage pattern of any terrain displays the features of the earth as well as subsurface formations. This characteristic, which can be recognized by the underlying lithology, is a key indicator of the rate of water percolation. Lithology, which is a key indicator of the natural drainage rate, determines the drainage network. Since it is influenced by factors including starting slope, variations in rock resistance, structural controls, recent deformation, and morphological changes, the drainage pattern is especially helpful in examining geomorphic properties and tracing the evolution of landforms. Data were taken from a DEM map and entered into a GIS program. Figure 4 shows the drainage density map of the Srivaikundam region. Five categories, ranging from very low (1) to very high, are used to categorize the drainage density in the studied area. The drainage density of the area is

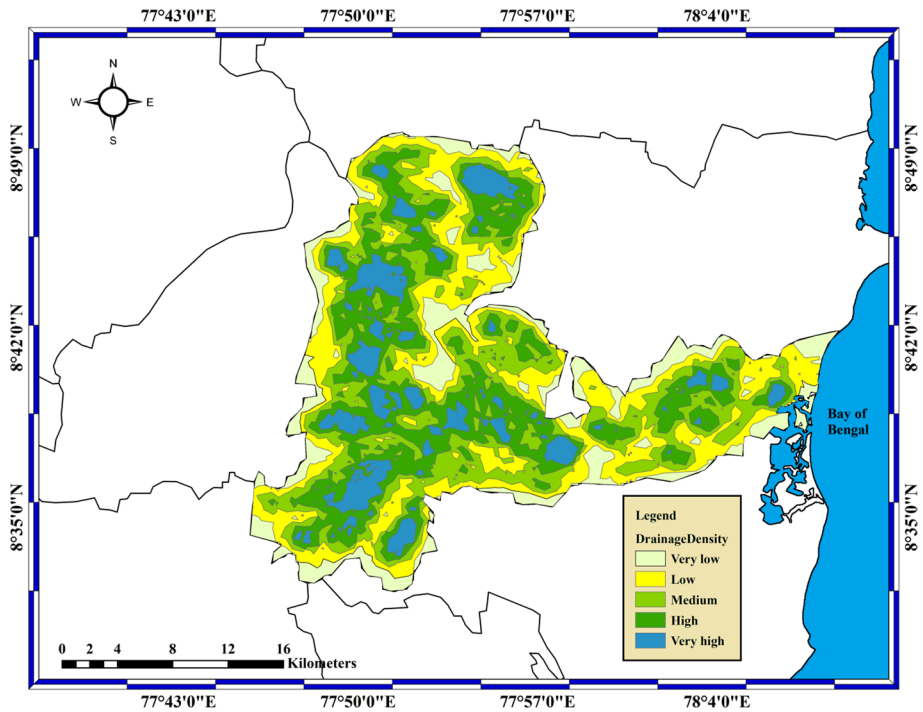


**Fig. 4** Drainage density map of Srivaikundam region

divided into five categories for the purposes of ranking. It has 5 different types. Extremely low to extremely high in terms of coverage, each kind has a percentage of 13.9% (very low), 24.6% (low), 26% (medium), 26% (high), and 10.1% (very high), respectively.

### 4.3 TWI (topographic wetness index) map

The topographic wetness index (TWI) gauges both the flow accumulation at each location in a drainage basin and the water's ability to flow down a slope gravitationally (Fig. 5). This parameter relates to the state of soil moisture, according to Gokceoglu et al. (2005).

$$TWI = Ln \frac{a}{\tan(\beta)} \quad (3)$$

Adding the area ( $a$ ) and the length ( $L$ ), where  $L$  is the slope in degrees, yields the catchment area. The slope angle of the location is given by  $\tan$ , and the entire upslope region drains through a point (per unit contour length). TWI has been used as an environmental correlate of the spatial variability of factors such as soil organic matter, soil nutrients, soil texture, and other soil parameters in soil investigations. TWI can be estimated using numerous procedures for both the catchment area (the numerator) and slope. The researchers determined that the choice of flow algorithm was the most influential choice in terms

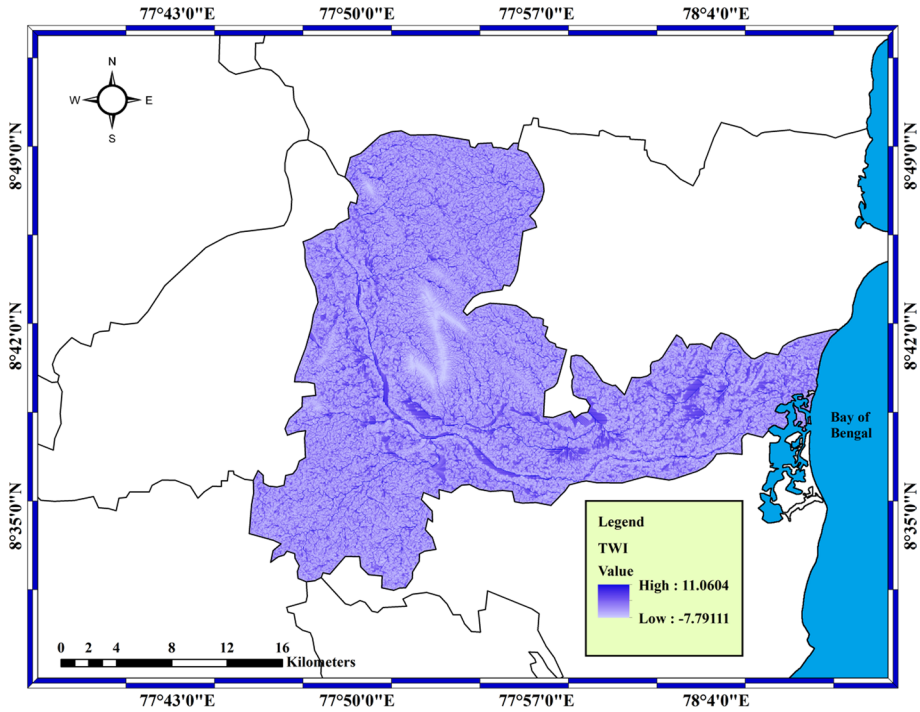


Fig. 5 TWI (topography weightage index) map by GIS method in the study area

of the connection between TWI and observed soil moisture after testing the sensitivity of the TWI to an exhaustive selection of flow algorithms and slope calculation methods. The TWI map was created in ArcGIS for this investigation and manually classified into five categories ranging from extremely low to high (Fig. 5).

#### 4.4 Distance from river map

Determining the flood-spreading region may involve taking the distance from the rivers into account. When floods start as a result of overflow, the areas closest to these rivers are the most severely affected. Floods are more likely in areas with a lot of surface water and near rivers. Flooding starts in the riverbeds and spreads throughout the surrounding area. As a result, when determining the flood potential zone, the distance from the rivers is given substantial weight. The water flows from higher altitudes and accumulates at lower elevations in the river basin, making the area around rivers more susceptible to flooding in both regular and flash flood conditions. During unusually heavy rains, dams, ponds, lakes, and the terrain around them are frequently swamped. This map was made in ArcGIS software using the buffering approach in Fig. 6.

#### 4.5 River length map

The ArcGIS tool can determine the length of the river or the flow length. The river flow is calculated so that flooding begins in the riverbeds and spreads to the surrounding land.

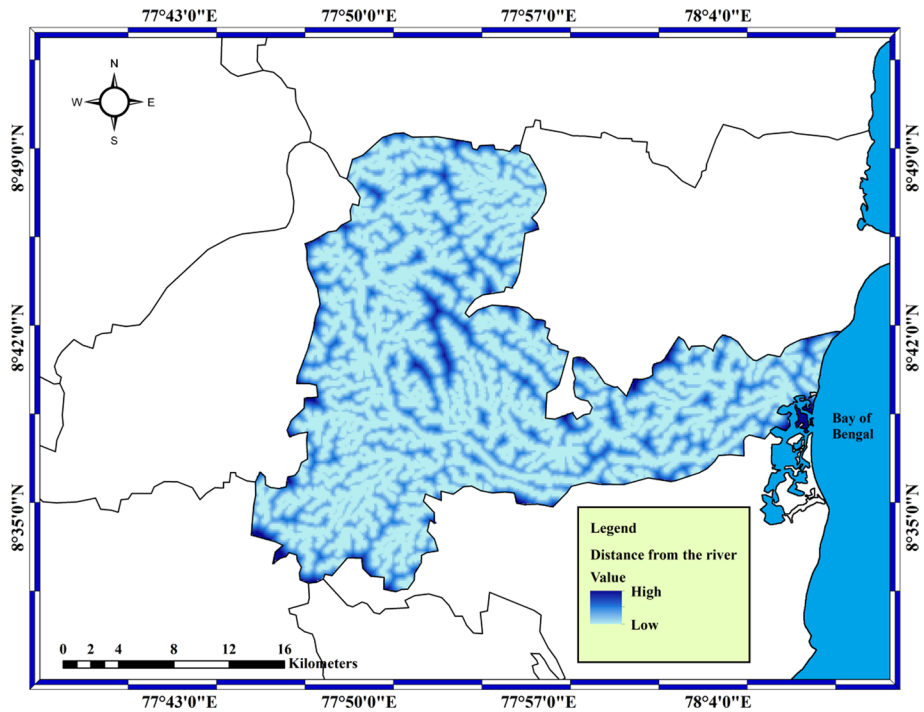


**Fig. 6** Distance from the river map by GIS method in the study area

Flow length is the horizontal projection length of the maximum surface distance along the flow direction from a point on the surface to the beginning of the stream. In recent years, river length has caught the attention of researchers. For many computations in river geomorphology, determining the exact length of a river is necessary. In the past, river length has been measured in the field or by analyzing vector-based topographic data in Shrivastava et al. (2018); Nath and Saha (2018). The length of a stream is the distance along the stream channel measured from the source to a certain region or to the exit; this distance can be measured on a map, as shown in Fig. 7.

#### 4.6 Slope map

The loss (or gain) in height per unit horizontal distance in a direction can be used to calculate the slope of the terrain investigated by Nagaraju et al. (2011). The slope of the land regulates infiltration and runoff. Since it affects the rate of infiltration and water retention, the land slope is an essential consideration in water exploration and development. The slope of a surface is the change in height across an area of the surface. The slope is a crucial factor that impacts the stability of the surface. Raster data were collected from the USGS website and utilized using the ArcGIS tool to categorize the slope variation map in this study area. Except for the southern region, which is steep, the terrain is mostly flat. A steeply sloping topography generates greater runoff and less infiltration, resulting in poor

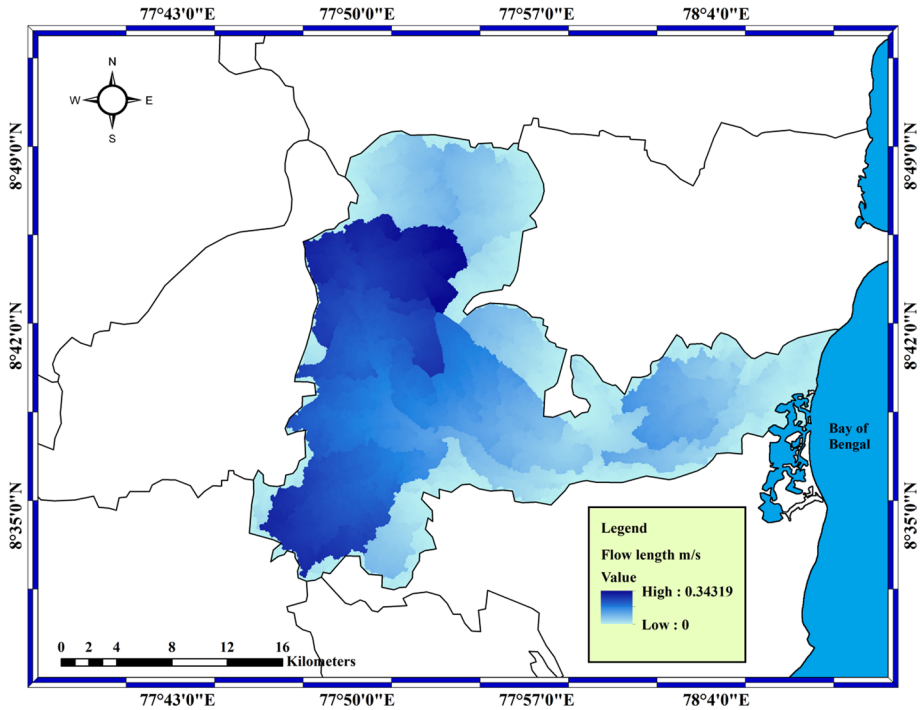
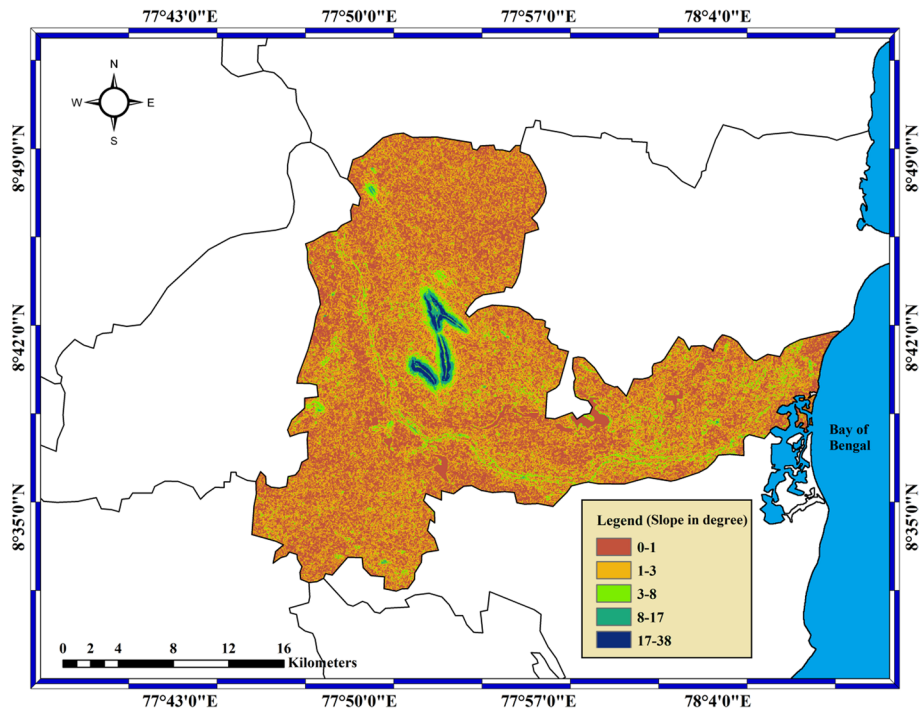


Fig. 7 Flow length map by GIS method in the study area

water quality. The slope of the research area was separated into five groups in order to apply weights (Fig. 8). It has 5 different types. Extremes of low and high in 37.9% (very low), 50.7% (low), 9.9% (middle), 1% (high), and 0.6% (very high) are the respective percentages of coverage for each kind.

#### 4.7 Digital elevation map

A digital elevation model (DEM) represents an elevation of the ground surface in relation to any vertical datum. DEM is a common name for any digital representation of a topographic surface (Fig. 9). The most fundamental form of topographic digital representation is a DEM, as studied by Sudalaimuthu et al. (2022). Elevation refers to the local and regional topography and offers details on the overall direction of groundwater flow as well as its impact on groundwater recharge and discharge. For the purpose of creating an elevation map for the chosen research area, the digital elevation map was acquired from the USGS website and imported as raster or STRM (DEM) satellite image data into the GIS environment. According to the map, the elevation of the Srivaikundam region ranges from – 14 m at the lowest point to 311 m at its highest point.



**Fig. 8** Slope map by GIS method in the study area

#### 4.8 Rainfall map

Flooding in lowland locations is mostly caused by runoff from rainfall, which is the primary supply of water for the earth's surface. Runoff occurs when rainfall exceeds the soil's and weathered rock's capacity to absorb water. Both the northeastern and southwesterly monsoons bring rain to the region. The Indian Meteorological Department (IMD) provided the data that was used to produce the study rainfall map by Rangarajan et al. (2019). The spatial interpolation method IDW was used to create the rainfall map once the data were imported into the GIS system. Rainfall in the area is divided into five categories for the purpose of ranking. It has five different types. Extremes of low and high (Fig. 10) in each variety have a different percentage coverage, which is as follows: 22.1% (very low), 23.9% (low), 15% (medium), 16.8% (high), and 22% (very high).

#### 4.9 Flood susceptibility map

The weighting approach and AHP were used to create the eight maps, which were then integrated and overlapped in the (GIS) environment (Subbarayan and Sivaranjani 2017). The identification of locations that are vulnerable to flooding is supported by the flood susceptibility map, and historical flood data attest to the correctness of the methodology (Samanta et al. 2018). The final map of the flood-sensitive area was created and divided into five main flood potentiality classes, ranging from extremely low to very high in Table 7.

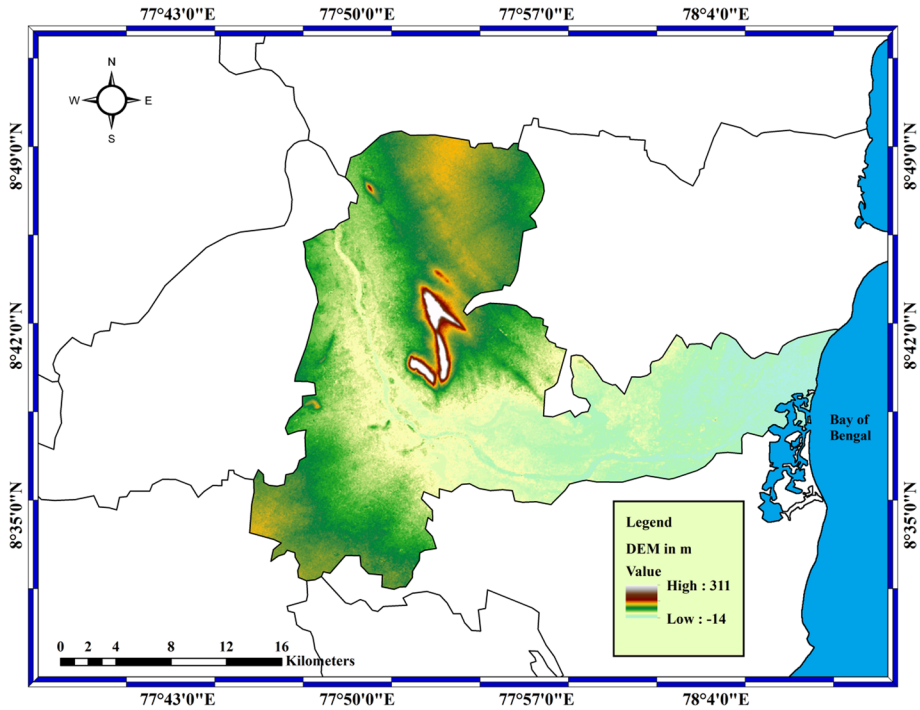


Fig. 9 DEM map by GIS method in the study area

According to the weights derived by the AHP approach, the study parameters are linearly included. In a GIS environment based on Eq. (4), the thematic layers are overlaid with various weights. The FSI was then calculated for every pixel contained within the study region. *R* is an Ranking, and *W* is an Weightage of the thematic layers

$$\begin{aligned}
 \text{FSI} = & R_{\text{LULC}} * W_{\text{LULC}} + R_{\text{DD}} * W_{\text{DD}} + R_{\text{TWI}} * W_{\text{TWI}} + R_{\text{DR}} * W_{\text{DR}} \\
 & + R_{\text{RL}} * W_{\text{RL}} + R_{\text{SI}} * W_{\text{SI}} + R_{\text{DEM}} * W_{\text{DEM}} + R_{\text{Rain}} * W_{\text{Rain}}
 \end{aligned}
 \tag{4}$$

They find that study area is very low class 1.7%, low class 26.3%, 42.1% of the area is in the medium class, 24% of the area is in the high class, and 5.9% of the area is in the very high class (Fig. 11). The flooding phenomenon is not significantly affected by these parameters, which are given the lightest weights. As a result, these results offer baseline data that must be taken into account during flood management.

### 5 Conclusion

The study objective was to investigate the areas of the Srivaikundam area that are vulnerable to flooding as a means of identifying disaster mitigation strategies. Flood disaster vulnerable zone mapping is one of the most constructive approaches for reducing flood hazard damages and assisting planners, stakeholders, and decision-makers in having effective supervision over flood-prone areas, thereby ensuring proper and sustainable socioeconomic development. As a result, the FSI was determined for each and every

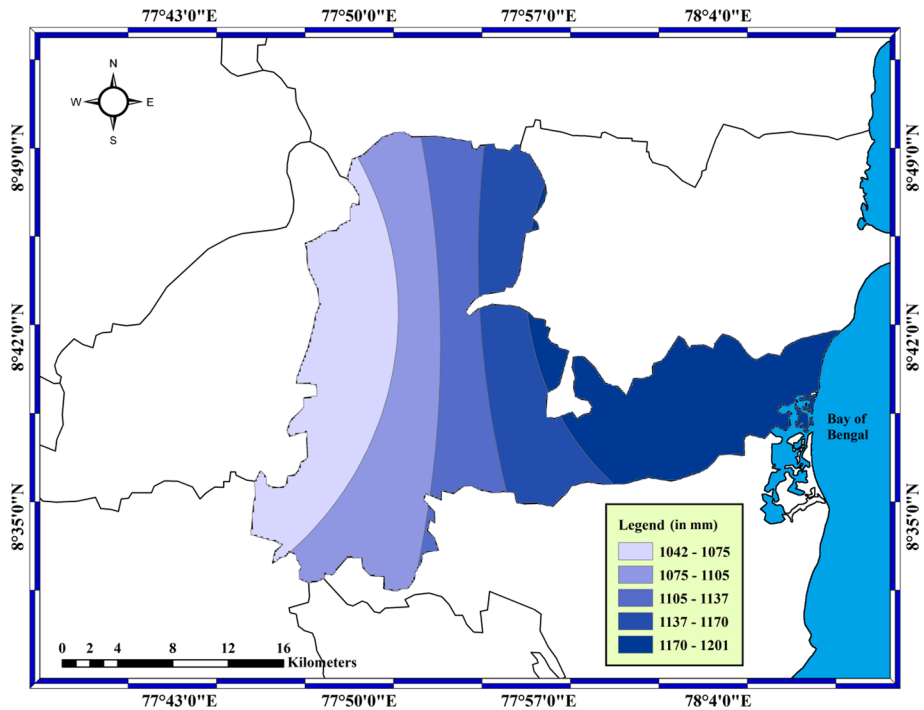


**Fig. 10** Rainfall map by GIS method in the study area

**Table 7** Classification of flood susceptibility zone

Classification	Total area covered	Area percentage (%)
Very low	9.54	1.7
Low	171.2	26.3
Medium	272.8	42.1
High	159	24
Very high	32	5.9

pixel in the research area. The appropriate scores were given to each class in order to determine the risk zone. The final suitability model results are considered acceptable for area planners and disaster management organizations to manage and reduce flood damages. The recommended map can be used by planners and decision-makers to help with both land use and water resource management and planning. Flood susceptibility maps, in particular, can be useful for identifying areas where urbanization expansion should be closely monitored or regulated in order to avoid potential future flood damage and losses. This study can be utilized by urban authorities to incorporate flood susceptibility



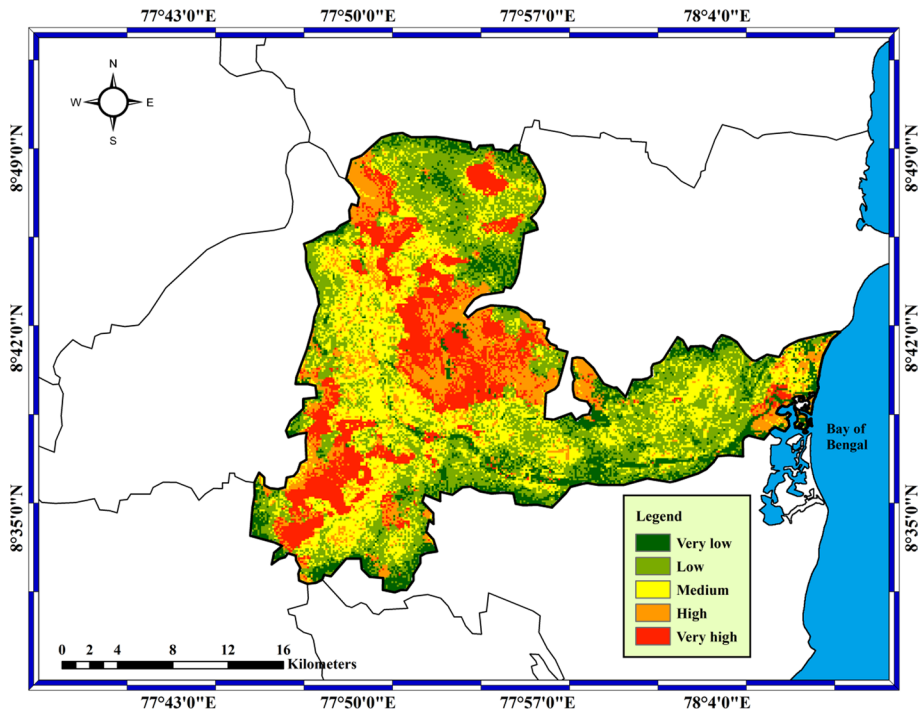


**Fig. 11** Flood susceptibility map of the study area

into detailed urban plans and land use planning projects in order to minimize the damage to lives and infrastructure. In future studies, it is advised that more flood and non-flood points be included, in addition to maps of flood-influencing elements at higher scales and geographic resolutions, which may affect the accuracy of the flood susceptibility mapping results. If they live in moderate or high flood plains or are otherwise vulnerable to flooding, the people should be made aware of the necessary safety actions to be taken prior to the flood occurrence.

**Acknowledgements** The First author expresses his sincere thanks to Shri. A.P.C.V. Chockalingam, Secretary and our Principal Dr. C. VeeraBhahu, V.O.Chidambaram College, Thoothukudi. The help was extended by Dr. P. Sivasubramanian, Professor and Head, PG and Research Department of Geology, V.O.Chidambaram College, Thoothukudi.

**Author contributions** RAS was involved in conceptualization and methodology, writing—original draft preparation and writing—review and editing. ARA contributed to supervision, writing—review and editing and resources.

**Funding** There is no funding source for this study.

## Declarations

**Conflict of interest** The authors declare that they have no conflict of interest.

**Consent to participate** Not applicable.

**Consent to publish** Not applicable.

**Ethical approval.** Not applicable.

## References

- Abdel Hamid HT, Wenlong W, Qiaomin L (2020) Environmental sensitivity of flash flood hazard using geospatial techniques. *Glob J Environ Sci Manag* 6(1):31–46
- Ahmed A, Hewa G, Alrajhi A (2021) Flood susceptibility mapping using a geomorphometric approach in South Australian basins. *Nat Hazards* 106(1):629–653. <https://doi.org/10.1007/s11069-020-04481-z>
- Bajabaa S, Masoud M, Al-Amri N (2014) Flash flood hazard mapping based on quantitative hydrology, geomorphology and GIS techniques (case study of Wadi Al Lith, Saudi Arabia). *Arab J Geosci* 7:2469–2481. <https://doi.org/10.1007/s12517-013-0941-2>
- Dandapat K, Panda GK (2017) Flood vulnerability analysis and risk assessment using analytical hierarchy process. *Model Earth Syst Environ* 3:1627–1646. <https://doi.org/10.1007/s40808-017-0388-7>
- Das S (2020) Flood susceptibility mapping of the Western Ghat coastal belt using multi-source geospatial data and analytical hierarchy process (AHP). *Remote Sens Appl Soc Environ*. <https://doi.org/10.1016/j.rsase.2020.100379>
- Elkhrachy I (2015) Flash flood hazard mapping using satellite images and GIS tools: a case study of Najran City, Kingdom of Saudi Arabia (KSA). *Egypt J Remote Sens Space Sci* 18(2):261–278. <https://doi.org/10.1016/j.ejrs.2015.06.007>
- Ghosh A, Kar SK (2018) Application of analytical hierarchy process (AHP) for flood risk assessment: a case study in Malda district of West Bengal. *India Nat Hazards* 94(1):349–368. <https://doi.org/10.1007/s11069-018-3392-y>
- Gokceoglu C, Sonmez H, Nefeslioglu HA, Duman TY, Can T (2005) The 17 March 2005 Kuzulu landslide (Sivas, Turkey) and landslide-susceptibility map of its near vicinity. *Eng Geol* 81(1):65–83
- Hammami S, Zouhri L, Souissi D, Souei A, Zghibi A, Marzougui A, Dlala M (2019) Application of the GIS based multi-criteria decision analysis and analytical hierarchy process (AHP) in the flood susceptibility mapping (Tunisia). *Arab J Geosci* 12(21):1–16. <https://doi.org/10.1007/s12517-019-4754-9>
- Hong H, Tsangaratos P, Ilia I, Liu J, Zhu AX, Chen W (2018) Application of fuzzy weight of evidence and data mining techniques in construction of flood susceptibility map of Poyang County, China. *Sci Total Environ* 625:575–588. <https://doi.org/10.1016/j.scitotenv.2017.12.256>
- Khosravi K, Nohani E, Maroufinia E, Pourghasemi HR (2016) A GIS-based flood susceptibility assessment and its mapping in Iran: a comparison between frequency ratio and weights-of-evidence bivariate statistical models with multi-criteria decision-making technique. *Nat Hazards* 83(2):947–987. <https://doi.org/10.1007/s11069-016-2357-2>
- Malik S, Pal SC, Das B, Chakraborty R (2020) Assessment of vegetation status of Sali River basin, a tributary of Damodar River in Bankura District, West Bengal, using satellite data. *Environ Dev Sustain* 22(6):5651–5685. <https://doi.org/10.1007/s10668-019-00444-y>
- Nagaraju K, Varma PST, Varma BR (2011) A current-slope based fault detector for digital relays. In: 2011 Annual IEEE India conference, pp 1–4. IEEE
- Natarajan L, Usha T, Gowrappan M, Palpanabhan Kasthuri B, Moorthy P, Chokkalingam L (2021) Flood susceptibility analysis in Chennai corporation using frequency ratio model. *J Indian Soc Remote Sens* 49(7):1533–1543. <https://doi.org/10.1007/s12524-021-01331-8>
- Nath A, Saha G (2018) River length calculation using map data. In: Proceedings of the international conference on computing and communication systems: I3CS 2016, NEHU, Shillong, India. pp 821–828. Springer, Singapore. [https://doi.org/10.1007/978-981-10-6890-4\\_78](https://doi.org/10.1007/978-981-10-6890-4_78)
- Rangarajan S, Thattai D, Cherukuri A, Borah TA, Joseph JK, Subbiah A (2019) A detailed statistical analysis of rainfall of Thoothukudi district in Tamil Nadu (India). In: Water resources and environmental engineering II. Springer, Singapore, pp 1–14. [https://doi.org/10.1007/978-981-13-2038-5\\_1](https://doi.org/10.1007/978-981-13-2038-5_1)
- Saaty TL (1980) The analytical hierarchy process. McGraw-Hill, New York
- Samanta S, Pal DK, Palsamanta B (2018) Flood susceptibility analysis through remote sensing, GIS and frequency ratio model. *Appl Water Sci* 8(2):1–14. <https://doi.org/10.1007/s13201-018-0710-1>
- Shrivastava D, Nath, A, Saha G (2018) River length calculation using map data. In: Proceedings of the international conference on computing and communication systems: I3CS 2016, NEHU, Shillong, India. Springer Singapore, pp 821–828
- Subbarayan S, Sivaranjani S (2017) Modelling of flood susceptibility based on GIS and analytical hierarchy process—a case study of Adayar River Basin, Tamilnadu, India. In: International expert forum: mainstreaming resilience and disaster risk reduction in education. Springer, Singapore, pp 91–110. [https://doi.org/10.1007/978-981-32-9527-8\\_6](https://doi.org/10.1007/978-981-32-9527-8_6)

- Sudalaimuthu K, Jesudhas CJ, Ramachandran U, Somanathan AK, Ganapathy S, Jeyakumar RB (2022) Development of digital elevation model for assessment of flood vulnerable areas using Cartosat-1 and GIS at Thimbarani river, Tamilnadu, India. *Environ Qual Manag.* <https://doi.org/10.1002/tqem.21842>
- Swain KC, Singha C, Nayak L (2020) Flood susceptibility mapping through the GIS-AHP technique using the cloud. *ISPRS Int J Geo Inf* 9(12):720. <https://doi.org/10.3390/ijgi9120720>
- Yaralıoğlu K (2004) Analitik Hiyerarşi Proses. Uygulamada Karar Destek Yöntemleri, İlkem Ofset, İzmir

**Publisher's Note** Springer Nature remains neutral with regard to jurisdictional claims in published maps and institutional affiliations.

Springer Nature or its licensor (e.g. a society or other partner) holds exclusive rights to this article under a publishing agreement with the author(s) or other rightsholder(s); author self-archiving of the accepted manuscript version of this article is solely governed by the terms of such publishing agreement and applicable law.